Journal of The Electrochemical Society, **149** (3) A288-A292 (2002)
0013-4651/2002/149(3)/A288/5/$7.00 © The Electrochemical Society, Inc.

The Effect of a Metal-Oxide Coating on the Cycling Behavior at 55°C in Orthorhombic $LiMnO_2$ Cathode Materials

Jaephil Cho,[a,*,z] Tae-Joon Kim,[b,] and Byungwoo Park[b,*]**

[a]*Samsung SDI Company, Limited, Energy Development Team, Chonan, Chungchongnam-Do, Korea*
[b]*School of Materials Science and Engineering, Seoul National University, Seoul, Korea*

The structural stability of metal-oxide-coated orthorhombic $LiMnO_2$ (o-$LiMnO_2$) was characterized by its 55°C cycling behavior. Sol-gel coating of the metal oxides (Al_2O_3 and CoO), followed by heat-treatment at 400°C, leads to the formation of the solid-solution layer ($LiMn_{1-x}M_xO_2$) with a concentration gradient of metal atoms at the particle surface. The specific capacity and cycle life at 55°C are influenced significantly by the metal-oxide coating. CoO-coated $LiMnO_2$ exhibits an additional voltage plateau at the deep discharge (2 V), and has a higher capacity than Al_2O_3-coated electrode, although the capacity retention is inferior to the Al_2O_3-coated cathode.
 [DOI: 10.1149/1.1446870]

Manuscript submitted April 2, 2001; revised manuscript received October 8, 2001. Available electronically January 29, 2002.

$Li_xMn_2O_4$ [LiB2 × 4] cathode materials have been studied intensively over the last 20 years as a potential application to Li batteries due to their low cost and environmental friendliness. The structure of spinel $LiMn_2O_4$ consists of a cubic-close-packed oxygen array where the lithium ions are located at the 8*a* tetrahedral sites and the manganese ions at the 16*d* octahedral sites of a cubic unit cell with space group $Fd3m$; the oxygen ions are located at the 32*e* positions.[1] When used as an insertion electrode in Li/$Li_xMn_2O_4$ cells, the lithium ions remain in the tetrahedral sites within a cubic structure for the range $0 < x \leqslant 1$; this reaction occurs at approximately 4 V *vs.* lithium metal. On the other hand, the insertion of lithium into octahedral sites in $Li_xMn_2O_4$ occurs at 3 V for $1 < x \leqslant 2$.[1] This causes a first-order transition to a rock-salt-phase $Li_2Mn_2O_4$ during which the tetrahedrally coordinated lithium ions are cooperatively displaced into the octahedral sites (16*c*). The increase in the Mn^{3+} concentration within the spinel framework in $Li_2Mn_2O_4$ reduces the crystal symmetry from cubic in $LiMn_2O_4$ to tetragonal ($I4_1/amd$).[1,2] The large anisotropic (Jahn-Teller) distortion ($c/a = 1.16$) is generally believed to be largely responsible for poor capacity retention of the spinel electrodes at 3 V. Mn dissolution from the spinel is also responsible for the decreased capacity, leading to the formation of defect-type spinels, as identified by the peak broadening in the X-ray diffraction (XRD) pattern.[3,4] Improved capacity retention can be achieved by substituting some of the Mn ions in the B2 × 4 spinel framework with monovalent, divalent, or trivalent cations. This substitution increases the average oxidation state of the spinel above 3.5 V.[2]

In contrast to $Li_xMn_2O_4$, o-$LiMnO_2$ has shown better cycle life performance than $LiMn_2O_4$ when both 3 and 4 V plateaus are utilized at room-temperature cycling.[5] However, the capacity loss was apparently enhanced at 55°C cycling, showing its capacity from maximum 180 to 80 mAh/g after 100 cycles between 4.4 and 2 V.[6] To minimize capacity fading, the $LiMn_{1-x}Al_xO_2$ system was studied. However, it cannot completely prevent Mn dissolution from the particle surface (electrolyte interface). Moreover, it decreased the original capacity by 30 mAh/g (from 180 to 150 mAh/g). In particular, a sol-gel coating of $LiCoO_2$ on the $LiMn_2O_4$ particles and subsequent heat-treatment at 800°C improved structural stability of the cathode. This was associated with the $LiMn_{2-x}Co_xO_4$-phase formation across the particle with discretely higher Co concentration at the particle surface than in the bulk.[7] A similar structural stability was observed in $LiCoO_2$ by using Al_2O_3 and SnO_2 coating.[8-10]

In this paper, we report the effect of a metal-oxide (CoO and Al_2O_3) coating on the cycling behavior at 55° in o-$LiMnO_2$ cathode particles.

Experimental

The o-$LiMnO_2$ powders were prepared from a stoichiometric mixture of $LiOH \cdot H_2O$ and Mn_2O_3 (1.05:1 mol ratio) after heating at 800°C for 24 h under Ar atmosphere. Both $Li_2Mn_2O_4$ and Li_2MnO_2 were prepared by chemical lithiation of $LiMn_2O_4$ with an excess of *n*-butyllithium in hexane at 50°C for 3 and 7 days, respectively. The reaction was carried out in an argon-filled glove box in which the residual water content was less than 9 ppm. After the reaction, the product was thoroughly rinsed with hexane, dried under vacuum, and stored in the glove box. Powders that were prepared at 50°C for 5 days showed a light brown color with a Li:Mn molar ratio of 1.43, as determined by inductively coupled plasma (ICP) mass spectroscopy.

Coatings of CoO and Al_2O_3 on the $LiMnO_2$ powder surface (with an average particle size of 13 μm) were performed as follows. Aluminum and cobalt ethylhexanodiisopropoxide $M(OOC_8H_{15})(OC_3H_7)_2$ (M = Al or Co) were first dissolved in isopropanol, followed by continuous stirring for 20 h at 21°C. This solution was then mixed with the powders such that the solution corresponded to 15 wt % of used o-$LiMnO_2$ powders. (The mole ratios of total Al and Co *vs.* Mn were 0.05 and 0.04, respectively). The mixture was further aged at 50°C in order to ensure good bonding between the M-OR groups and o-$LiMnO_2$ surface-OH groups. After the o-$LiMnO_2$ powders were dried for 10 h at 150°C, the batches were fired at 400°C for 10 h. The surface area before and after coating was 1.3 and 1.5 m^2/g, respectively. For electrochemical testing, cathode slurry was prepared by mixing the oxide powders, carbon black (Super P), and poly(vinylidene) fluoride (PVDF) in a weight ratio of 92:4:4. The coin-type cells (2016 size) contained the o-$LiMnO_2$ powders, a polyethylene microfilm separator, and Li metal. The electrolyte was 1 M $LiPF_6$ dissolved in a mixture of ethylene carbonate/dimethyl carbonate (1/1 vol %). The XRD patterns after cycling were taken using electrodes that were prepared as follows. Cycling tests were stopped at the end of discharge at 2 V and held at this voltage for 20 h. The cells were then disassembled carefully in a glove box to remove the cathode. This cathode was subsequently washed with dimethyl carbonate (DMC) to remove the $LiPF_6$, followed by drying in a vacuum oven at 80°C for 24 h.

Results and Discussion

The XRD patterns of the standard compounds $LiMn_2O_4$, Li_2MnO_2, $Li_2Mn_2O_4$, and o-$LiMnO_2$ are shown in Fig. 1. The pattern of the o-$LiMnO_2$ can be easily distinguished from that of the tetragonal $Li_2Mn_2O_4$ ($I4_1/amd$). The o-$LiMnO_2$ phase has a dis-

* Electrochemical Society Active Member.
** Electrochemical Society Student Member.
z E-mail: jpcho@samsung.co.kr

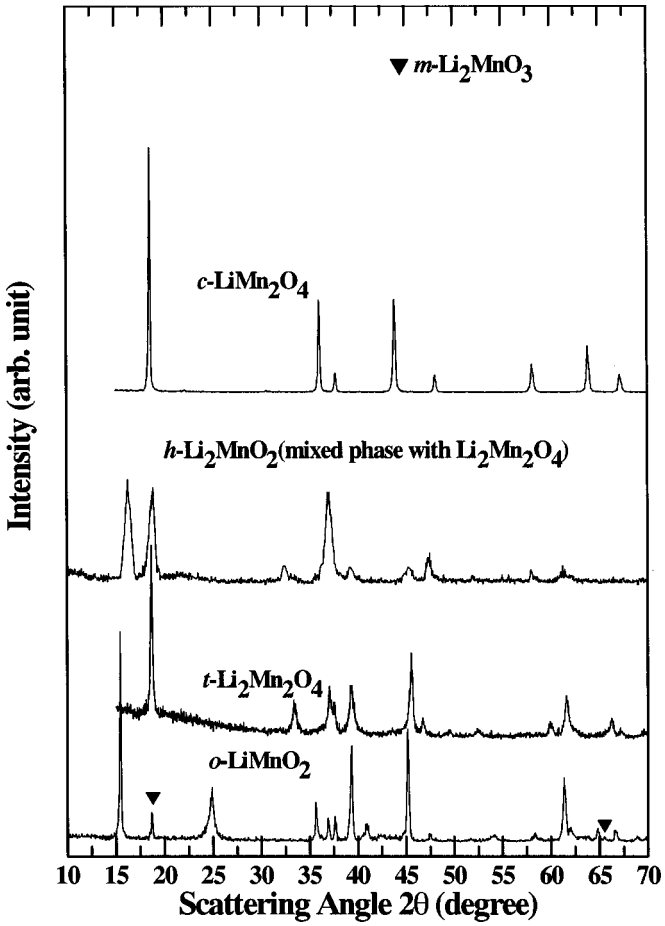

Figure 1. XRD patterns of $LiMn_2O_4$, Li_2MnO_2, $Li_2Mn_2O_4$, and *o*-$LiMnO_2$. The Li_2MnO_2 phases consist of a mixed phase with $Li_2Mn_2O_4$.

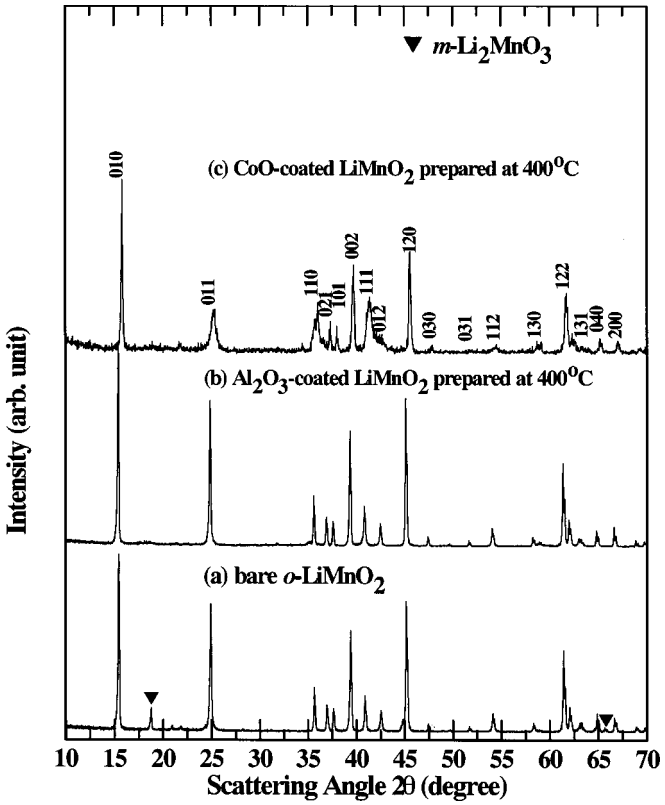

Figure 2. XRD Patterns of (a) bare $LiMnO_2$, (b) Al_2O_3-coated, and (c) CoO-coated $LiMnO_2$ materials. The coated cathodes were prepared at 400°C for 10 h.

torted cubic close-packed oxygen array with alternating zigzag layers of Li and Mn cations. No significant broadening of the XRD peaks from *o*-$LiMnO_2$ was observed, while a narrow (011) diffraction peak in the orthorhombic phase was correlated with planar stacking faults.[11] A full width at half-maximum (fwhm) in the (011) peak was 0.096°, indicating that the present material is in a well-ordered orthorhombic structure. The XRD pattern of the Li_2MnO_2 appears to indicate a substantial amount of $Li_2Mn_2O_4$-impurity phase, similar to that reported by David *et al.*[12] Although the XRD pattern of Li_2MnO_2 phase, which has $P3m1$ symmetry, is similar to that of $Li_2Mn_2O_4$, these two compounds can be distinguished from each other by the peak at ~16.2°, as shown in Fig. 1.

The XRD patterns of Al_2O_3- and CoO-coated *o*-$LiMnO_2$ prepared at 400°C were compared to that of the bare one, as shown in Fig. 2. While the fwhm of the Al_2O_3-coated *o*-$LiMnO_2$ is identical to that of the bare one ($2\theta \cong 0.096°$) for the (011) peak, CoO-coated $LiMnO_2$ showed increased fwhm to 0.15°, indicating the CoO coating increased the density of stacking faults, *i.e.*, structural disorder. This behavior can also be observed in the increased broadening of the (110) and (111) peaks. Other phenomena observed are the disappearance of the Li_2MnO_3 impurity phase after the metal-oxide coating. This is believed to be due to a decomposition reaction of Li_2MnO_3 with CoO or Al_2O_3 gels that occurs during heat-treatment at 400°C, and can result in the formation of $LiMnO_2$ and $LiMO_2$ (M = Co or Al). This implies that the Li_2MnO_3 phase was mainly distributed on the *o*-$LiMnO_2$ particle surfaces.

However, XRD does not distinguish whether the metal oxides remain on the particle surface, or have reacted with $LiMnO_2$. To analyze the concentration profile in depth, into the particle, coated samples were cross-sectioned, by polishing, for electron-probe microanalysis (EPMA), as shown in Fig. 3. The figure shows a significant amount of Al and Co atoms corresponding to, respectively, ~32 and ~27 atom %, within ~1 μm range from the surface. This suggests the formation of a solid solution ($LiMn_{1-x}M_xO_2$) at the surface. The metal oxides (Al_2O_3 and CoO) interdiffused with $LiMnO_2$ during heat-treatment, exhibiting concentration gradients of metal atoms at the particle surface. Additional analysis by Auger electron spectroscopy (AES) of Al_2O_3-coated sample confirms the solid-solution formation (inset in Fig. 3). Such solid-solution thin-film

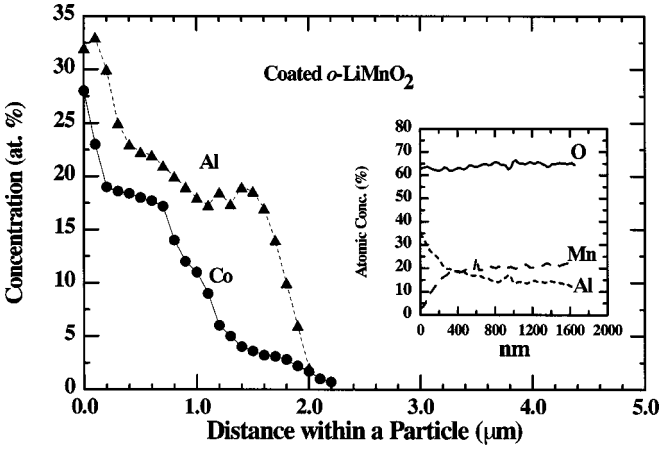

Figure 3. Plots of Al and Co concentration within a particle using an EPMA. The inset is a plot of Al_2O_3-coated sample using an AES.

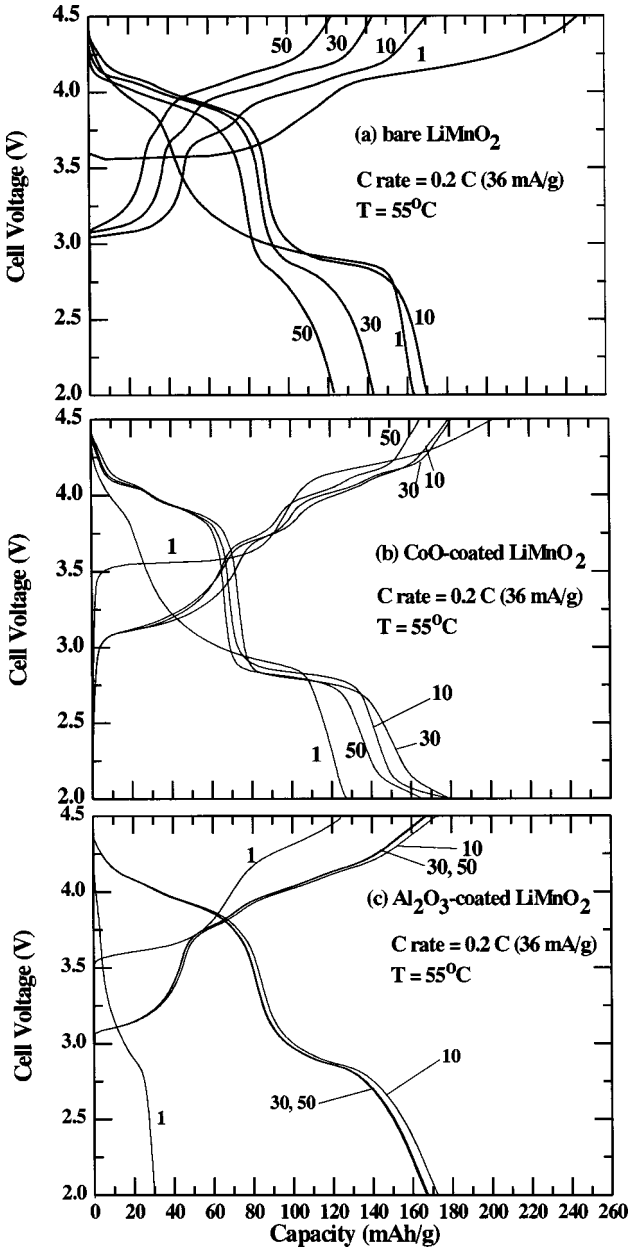

Figure 4. Plots of the voltage profile *vs.* capacity of (a) bare, (b) CoO-coated, and (c) Al_2O_3-coated $LiMnO_2$, after 1, 10, 30, and 50 cycles. The cell were cycling at the rate of 0.2 C (=36 mA/g) between 4.5 and 2 V at 55°C.

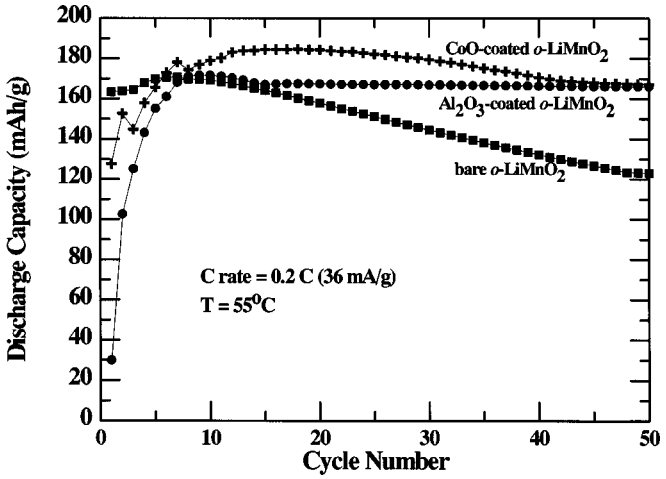

Figure 5. Plots of the discharge capacity *vs.* cycle number in bare, CoO-coated, and Al_2O_3-coated $LiMnO_2$ electrodes at the rate of 0.2 C (=36 mA/g) between 4.5 and 2 V at 55°C.

coating on the particle surface affects the overall lattice constants of *o*-$LiMnO_2$. The lattice constants *a*, *b*, and *c* for bare *o*-$LiMnO_2$ were calculated to be 2.806 ± 0.001, 5.756 ± 0.001, and 4.572 ± 0.001 Å, respectively, while those of the CoO-coated $LiMnO_2$ heat-treated at 400°C were 2.800 ± 0.001, 5.752 ± 0.001, and 4.567 ± 0.002 Å, respectively. On the other hand, those of the Al_2O_3-coated $LiMnO_2$ oxides prepared at 400°C were 2.802 ± 0.001, 5.754 ± 0.001, and 4.572 ± 0.002 Å, respectively.

Figure 4 compares the voltage profiles of the bare electrodes with the coated electrodes after 1, 10, 30, and 50 cycles. The first discharge capacities of Al_2O_3- and CoO-coated electrodes are smaller than that of bare one, showing 30 and 127 mAh/g, respectively. Such a difference may be attributed to the solid solution residing at the particle surfaces. However, discharge capacities of the coated electrodes after 10 cycles were similar to or even higher than that of uncoated cathode. Note that the discharge capacity of the CoO-coated electrode is higher than that of the bare and Al_2O_3-coated ones, showing 179 mAh/g after 10 cycles, which is due to the additional voltage plateau (near 2 V) at the end of discharge. This unique behavior cannot be observed in the bare and Al_2O_3-coated electrodes. In our case, the only difference between the Al_2O_3-and CoO-coated materials is the degree of structural disorder (as shown in Fig. 2), probably causing an additional voltage plateau. However, the capacity retention of the Al_2O_3-coated electrodes is superior to that of the CoO-coated electrode, showing only 2% capacity loss at the 50th cycle, as shown in Fig. 5. This shows that the Al_2O_3 coating is more effective in stabilizing the structural stability during cycling than the CoO coating.

To investigate the structural stability of the coated material, the changes in discharge capacities at 2 V (between 2.3 and 2.0 V), 3 V (between 3.5 and 2.3 V), and 4 V (between 4.5 and 3.5 V) regions are shown in Fig. 6. The discharge capacities of bare electrodes underwent a rather rapid capacity loss in both plateaus, especially decreasing from 117 to 46 mAh/g in the 3 V region after 50 cycles. The capacity fading of the 3 V region was attributed to the formation of the Li_2MnO_3 phase from $Li_2Mn_2O_4$.[13] In contrast, those of the Al_2O_3- and CoO-coated electrodes were apparently stabilized, but the overall capacity decay of the CoO-coated electrode is related to the capacity decrease of the 2 V plateau (2.3-2.0 V range). Note that Al substitution limits the amount of Li that can be inserted in the 3 V plateau, which accounts for the lower capacity. On the other hand, with Co substitution, capacity retention remains high in the 3.5-2.3 V range, compared to the 2.3-2.0 V range.

To support the evidence of structural degradation of the bare electrode, and to compare it with the coated electrodes, the cycled electrodes were disassembled from the coin cell, and XRD analysis was carried out, as shown in Fig. 7. XRD patterns differ from each other, but a common feature is that characteristic *o*-$LiMnO_2$ peak at 15° has disappeared in all the electrodes. In particular, monoclinic $LiMnO_2$ (*m*-$LiMnO_2$) phase formation in both the bare and CoO-coated samples indicates cycling-induced phase transformations. The bare electrodes consist mainly of cubic $LiMn_2O_4$ with a small amount of tetragonal $Li_2Mn_2O_4$, *m*-$LiMnO_2$, and Li_2MnO_3 phases. Since tetragonal $Li_2Mn_2O_4$ and *m*-$LiMnO_2$ have extremely similar XRD patterns, it is impossible to identify each phase from the cycled electrodes. In spite of this fact, we do not rule out the tetragonal $Li_2Mn_2O_4$ phase formation in the electrode, because a similar study by Chiang *et al.*[6] showed this. However, capacity fading due

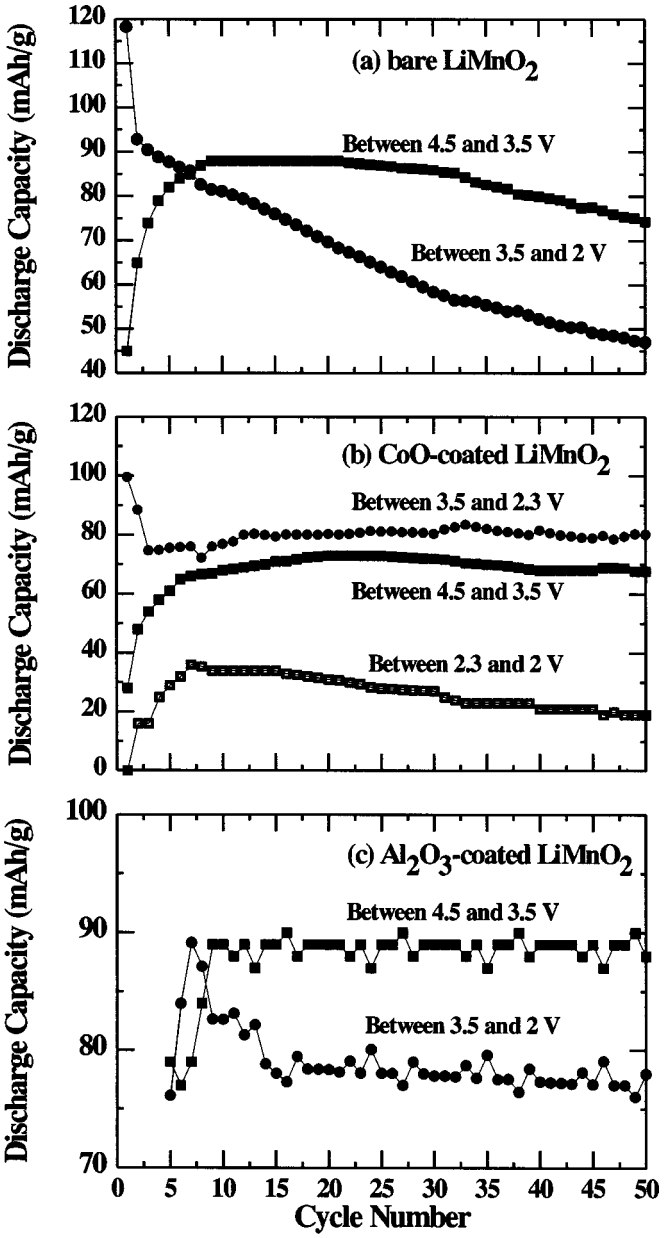

Figure 6. Discharge capacities at 4, 3, and 2 V plateau *vs.* cycle number for (a) bare, (b) CoO-coated, and (c) Al_2O_3-coated $LiMnO_2$.

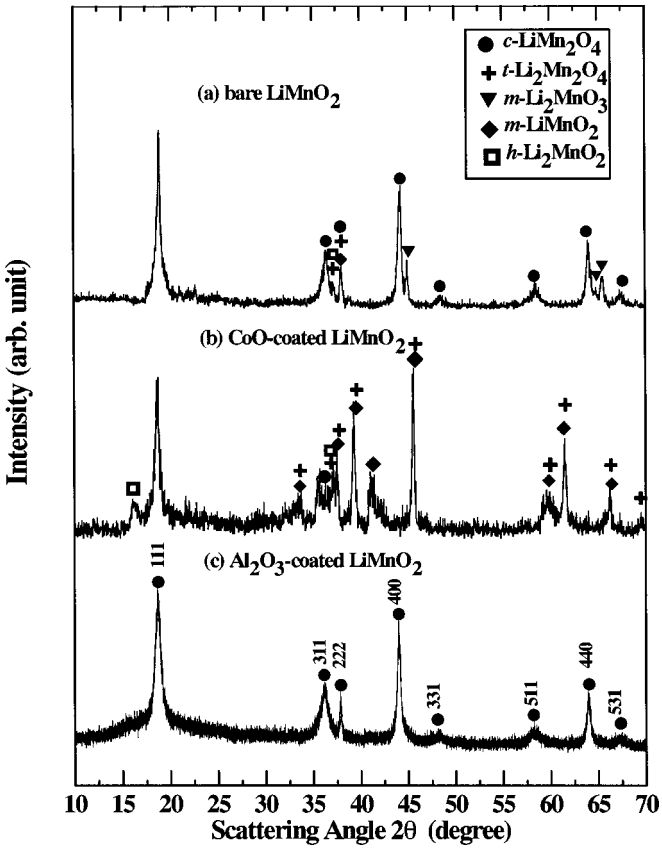

Figure 7. XRD patterns of (a) bare, (b) CoO-coated, and (c) Al_2O_3-coated $LiMnO_2$ electrodes after 50 cycles. The cycled CoO-coated electrodes also show some unidentified phases. After cycling, all cells were maintained for 20 h at 2 V at a constant voltage mode.

to Jahn-Teller (J-T) distortion seems to be negligible, compared to that from Mn dissolution from the $Li_2Mn_2O_4$. Because so many spinel phases exist in the Li-Mn-O ternary phase diagram, it is impossible to determine the exact phase and composition of electrodes from the XRD pattern alone.[14] However, the increased diffraction-peak broadening of the cubic $LiMn_2O_4$ confirms the formation of defect-type spinels. Dissolution of MnO into the electrolyte results in an increase in the Li:Mn ratio in the residual structure and a concomitant oxidation of Mn^{3+} to Mn^{4+}. The increased intensity of the Li_2MnO_3 peak at 65.5° supports the evidence that MnO is dissolved from $Li_2Mn_2O_4$.

Conversely, the XRD pattern of the CoO-coated electrode is different from that of the bare electrode in that $Li_2Mn_2O_4$ and *m*-$LiMnO_2$ are the major phases. In the case of Al_2O_3-coated $LiMnO_2$ electrode, the XRD pattern look much simpler, compared to both the bare and CoO-coated electrodes, showing only a cubic $LiMn_2O_4$ phase. The XRD pattern of the CoO-coated electrode shows a new peak at 16.2°, which has not been observed in other electrodes. While the exact phase cannot be identified by XRD alone, the position suggests the Li_2MnO_2 phase. Because the development of dislocations or structural defects on the particle surface can allow additional lithium intercalation, a solid-solution layer ($LiMn_{1-x}Co_xO_2$) could allow more lithium intercalation, leading to metastable $Li_2Mn_{1-x}Co_xO_2$ surface-layer formation. Similar behavior in $LiNiO_2$ was reported by Mueller-Neuhaus *et al.*[15] where they suggested that $Li_2Ni_{1-y}Fe_yO_2$ was formed on the surface of $Li_yNi_{1-y}Fe_yO_2$ cathode particles during deep discharge. The significant decrease in Li_2MnO_3 phase in both coated electrodes also confirms that a protective solid-solution layer minimizes Mn dissolution from $Li_2Mn_2O_4$.

XRD patterns of the Al_2O_3-coated electrodes after cycling show very broad diffraction-peak widths, which is related to the formation of local-lattice strains and small crystallites in the electrode powders during cycling. However, this differs from the case of the bare cathode, because the peak broadening there is mainly due to the Mn dissolution. To deduce these factors quantitatively, we analyzed five diffraction peaks, (111), (311), (222), (400), and (440). The XRD peak widths Δk (in fwhm) were fitted for each peak with scattering vector $k = (4\pi/\lambda)\sin\theta$, and a resolution function ($\Delta k_{resol} = 0.0046$ Å^{-1}) was subtracted after fitting each diffraction peak to take into consideration the instrumental broadening effect in diffraction.[16] As shown in Fig. 8, Δk has increased from $\Delta k = 0.0065 \pm 0.0021$ Å^{-1} (averaged from (010) up to (112) peaks) before cycling, to $\Delta k = 0.0328 \pm 0.0204$ Å^{-1} (averaged from (111) up to (440) peaks) after cycling in electrodes at 400°C, indicating that small crystallites (on the order of a few hundred

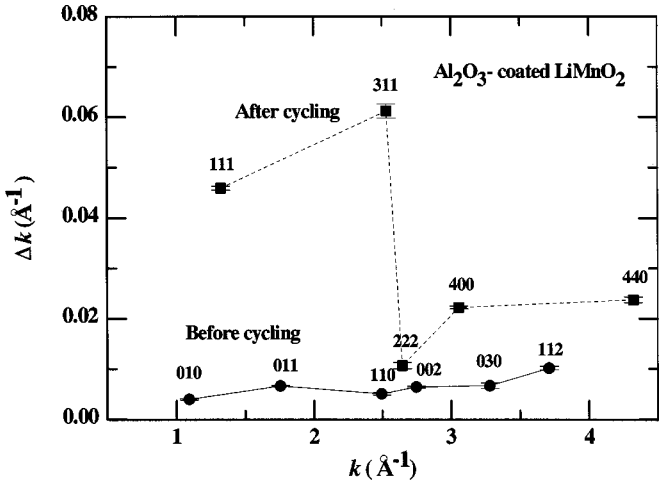

Figure 8. Plots of Δk *vs.* k in the Al_2O_3-coated $LiMnO_2$ electrode, before and after cycling.

angstroms) were developed during cycling. Even though there were insufficient cubic-spinel diffraction peaks in the XRD pattern of the CoO-coated $LiMnO_2$, similar Δk values in (111) diffraction peak between Al_2O_3- and CoO-coated electrodes indicate the formation of a similar crystallite/domain size and/or local strains. It has been proposed that the peak broadening could result from an inhibited transformation to a tetragonal spinel, or from the Li-concentration gradients within the particles.[5]

Conclusions

Capacity fading of bare $LiMnO_2$, which originated from Mn dissolution, was greatly reduced by a protective $LiMn_{1-x}M_xO_2$ (M = Al and Co) thin-film layer by a sol-gel coating of metal oxides with appropriate heat-treatments. While CoO-coated material showed higher degree of stacking faults with higher discharge capacity, the capacity retention was superior in Al_2O_3-coated $LiMnO_2$.

Acknowledgment

The authors thank Yong Jeong Kim at Seoul National University for XRD and AES measurements of Al_2O_3-coated samples. This work is supported by Samsung SDI and Korea Science & Engineering Foundation, through University-Industry Cooperative Program.

Seoul National University assisted in meeting the publication costs of this article.

References

1. J. M. Tarascon, E. Wang, F. K. Shokoohi, W. R. Mckinnon, and S. Colson, *J. Electrochem. Soc.*, **138**, 2859 (1991); and references therein.
2. A. D. Robertson, S. H. Lu, and W. F. Howard Jr., *Prog. Batteries Battery Mater.*, **16**, 20 (1997); and references therein.
3. A. Blyr, C. Sigala, G. G. Amatucci, D. Guyomard, Y. Chabre, and J. M. Tarascon, *J. Electrochem. Soc.*, **145**, 194 (1998).
4. J. Cho, *Solid State Ionics*, **138**, 267 (2001).
5. Y.-I. Jang, B. Huang, H. Wang, D. R. Sadoway, and Y.-M. Chiang, *J. Electrochem. Soc.*, **146**, 3217 (1999).
6. Y.-M. Chiang, D. R. Sadoway, Y.-I. Jang, B. Huang, and H. Wang, *Electrochem. Solid-State Lett.*, **2**, 107 (1999).
7. J. Cho, G. B. Kim, H. S. Lim, C.-S. Kim, and S.-I. Yoo, *Electrochem. Solid-State Lett.*, **2**, 607 (1999).
8. J. Cho, Y. J. Kim, and B. Park, *J. Electrochem. Soc.*, **148**, A1110 (2001).
9. J. Cho, Y. J. Kim, and B. Park, *Chem. Mater.*, **12**, 3788 (2000).
10. J. Cho, C.-S. Kim, and S.-I. Yoo, *Electrochem. Solid-State Lett.*, **3**, 362 (2000).
11. L. Croguennec, P. Deniard, R. Brec, and A. Lecerf, *J. Mater. Chem.*, **7**, 511 (1997).
12. W. I. F. David, J. B. Goodenough, M. M. Thackeray, and M. G. S. R. Thomas, *Rev. Chim. Miner.*, **20**, 636 (1983).
13. J. Cho and M. M. Thackeray, *J. Electrochem. Soc.*, **146**, 3577 (1999).
14. M. M. Thackeray, A. de Kock, M. H. Rossouw, D. Liles, R. Bittihn, and D. Hoge, *J. Electrochem. Soc.*, **139**, 363 (1992).
15. J. R. Mueller-Neuhaus, R. A. Dunlap, and J. R. Dahn, *J. Electrochem. Soc.*, **147**, 3598 (2000).
16. Y. Kim, J. Oh, T.-G. Kim, and B. Park, *Appl. Phys. Lett.*, **78**, 2363 (2001).